An Improved Zero-Voltage-Transition Technique in a Single-Phase Active Power Factor Correction Circuit

Suriya Kaewarsa

School of Electrical Engineering, Rajamangala University of Technology Isan Sakon Nakhon Campus, Sakon Nakhon, Thailand

Abstract

This paper presents an improved Zero-Voltage-Transition Technique (ZVT-Technique) in a single-phase active power factor correction circuit based on a dc-dc boost converter topology and operated in a continuous-inductor-current mode with fixed-switching frequency control. An additional circuit for reducing the turn-off switching loss of the auxiliary switching circuit was applied. Experimental work was carried out with a circuit operated at 220 V_{rms} *input voltage, 400* V_{dc} *output voltage, 500 W output power and 40 kHz switching frequency. The test results showed that the efficiency was improved from 95 to 97%t with the proposed circuitry, while the power factor was constant.*

Keywords: *Boost converter, dc-dc converter, power factor correction, soft-switching, boost converter topology, continuous-inductor-current mode.*

Introduction

In recent years, the number of rectifiers connected to utilities has increased rapidly, mainly due to the growing use of computers. Therefore, the problems caused by the harmonic currents become more important. International regulations governing the amount of harmonic currents (e.g. IEC1000-3-2) became mandatory and active power factor correction (PFC) circuit became inevitable for the ac-dc converters.

Generally, the solution for harmonic reduction and PFC are classified into passive approach and active approach. The passive approach offers the advantages of high reliability, high power handling capability and easy to design and maintain. However, the operation of passive compensation system is strongly dependent on the power system and does not achieve high power factor. While the passive approach remains the best choice in many high power applications, the active approach dominates the low to medium power applications due to their extraordinary performance (unity power factor and efficiency approach to 100%), regulation capabilities and high power density. With the power handling capability of power semiconductor devices being extended to megawatts, the active power electronic systems tend to replace most of the passive power processing devices (Akagi 1994; Bose 1992; McEachern 1990).

Today's harmonic and PFC technique to improve distortion are still under development. Power supply industries are undergoing the change of adopting more and more PFC techniques in all off-line power supplies. Moreover, with the residential and defense industries continuously demanding for even higher power density, switching mode power supply operating at high frequency is required because at high switching frequency, the size and weight of circuit components can be remarkably reduced. However, with the increasing of switching frequency, the switching loss becomes intolerable, resulting in very low conversion efficiency (Gegner and Lee 1994).

Soft-switching techniques have been widely used in reducing the switching losses and EMI noises of switching mode power converter. Soft-switching techniques, especially zero-voltage-transition (ZVT) have become more and more popular in the power supplies industries. The boost PFC converter employing the ZVT technique was first introduced by Hua *et al.* (1994) showed in Fig. 1. This converter provides ZVS condition for the main switch without increasing voltage stress of the active switches. However, it has a disadvantage such as the auxiliary switching circuit is turned-off with hard-switching which deteriorates the overall efficiency and increase EMI noises (Kim, *et al.* 2000).

This paper proposes an improved ZVT PWM boost PFC converter using additional circuit. The proposed converter achieves zero voltage or zero current turn-on and turn-off for the active switches as well as the soft-switching for the passive switches. A 500 W, 40 kHz ZVT PWM boost PFC converter prototype has been implemented to verify the improved performance of the proposed converter.

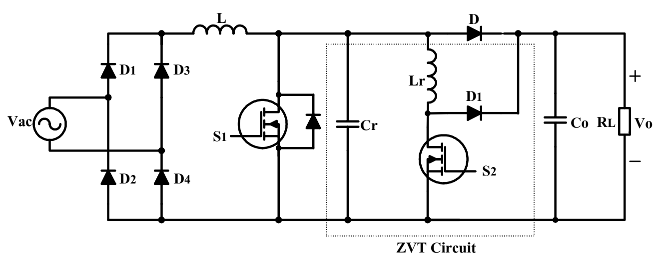

Fig. 1. Conventional ZVT PWM boost PFC converter

Circuit Description and Operation

The power stage of the proposed converter is shown in Fig. 2. The additional circuitry of the converter is consisted of a diode (D_2) and two capacitors (C_1, C_2). The converter operates in a continuous current mode with fixed frequency.

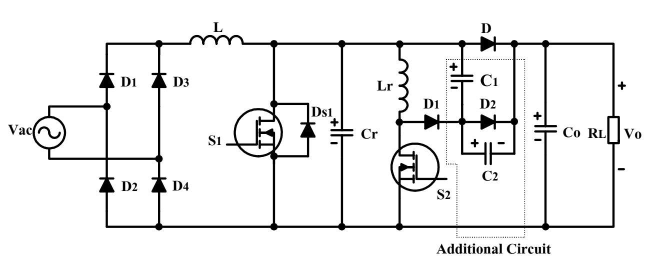

Fig. 2. Proposed ZVT PWM boost PFC converter

By inserting additional circuit, all of the switches, including auxiliary switches, are only turned-on and off at soft-switching.

The proposed converter has eight operating modes. The ideal waveform and equivalent circuit of each mode are shown in Figs. 3 and 4, respectively. To analyze the steady state operation, all components and devices are assumed to be ideal and the boost inductor (L) and output capacitor (C_o) are assumed to be large enough to treat as a current source and a voltage source, respectively (Kaewarsa, *et al.* 2004).

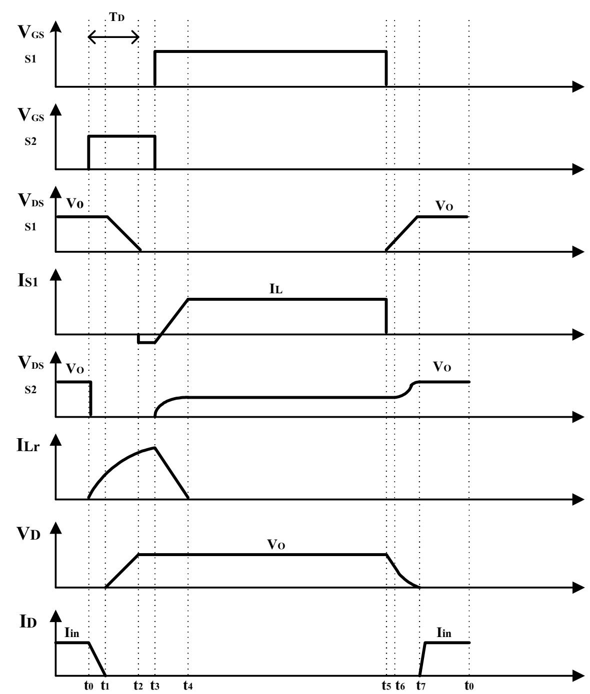

Fig. 3. Theoretical waveform of the proposed converter

Mode of Operation

The operations of each mode are explained as follows:

Mode 1 [$t_0 - t_1$]: Prior to $t = t_0$, the main switch S_1 and the auxiliary switch S_2 are turned-off, and main diode D is conducting. At $t = t_0$, S_2 is turned-on, the resonant inductor current I_{Lr} linearly ramp up until it reaches I_{in} at t_1, where main diode D is turned-off with soft-switching. The voltage and current expressions that govern this circuit mode are given by:

$$I_{Lr} = \frac{V_o}{L_r} t \qquad (1)$$

$$V_{Cr} = V_{Lr} = V_o \, . \qquad (2)$$

Mode 2 [$t_1 - t_2$]: At t_1, the resonant inductor current I_{Lr} reaches I_{in}, L_r and C_r begins to resonate. The resonant capacitor voltage V_{Cr} is equal to V_o. The voltage and current expressions are given by:

$$I_{Lr} = I_{in} + \frac{V_o}{Z_n} sin\omega_n (t - t_1) \qquad (3)$$

$$V_{Cr} = V_o \, cos\omega_n (t - t_1) \qquad (4)$$

where $Z_n = \sqrt{\frac{L_r}{C_r}}$ $\omega_n = \frac{1}{\sqrt{L_r C_r}}$.

Mode 3 [$t_2 - t_3$]: When V_{Cr} reaches zero the body diode D_{S1} of the main switch conducts providing a freewheeling way for L_r current. At this instant, main switch S_1 can be turned-on at zero voltage. The current I_{DS1} is given by:

$$I_{DS1} = \left(I_{in} + \frac{V_o}{Z_n} \right) - I_{in} = \frac{V_o}{Z_n} \, . \qquad (5)$$

Mode 4 [$t_3 - t_4$]: The auxiliary switch S_2 is turned-off witch near ZVS at $t = t_3$. The energy stored in the resonant inductor L_r is transferred to the capacitor C_1 and C_2. Then the voltage polarity of the capacitor C_1 is reversed to negative. During this period, the capacitor C_1 is acting as a turn-off snubber of the auxiliary switch. The energy stored in the capacitor C_2 will be recycled and used to suppress the turn-off voltage spike of the main switch S_1. The voltage and current expressions of this mode are given by:

$$I_{Lr} = I_{Lr}(t_2) cos\omega_n (t - t_3) \qquad (6)$$

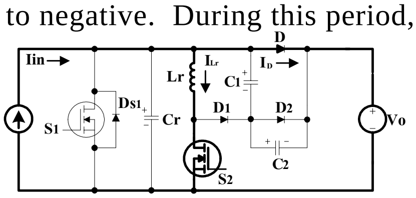

(a) Mode 1

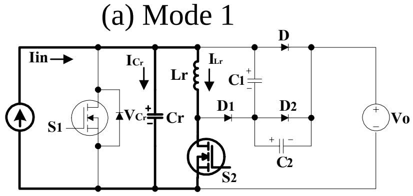

(b) Mode 2

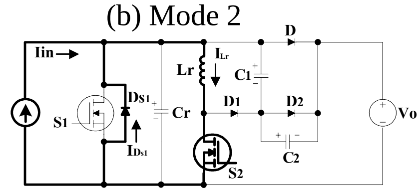

(c) Mode 3

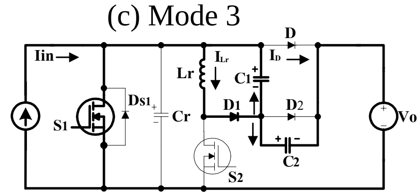

(d) Mode 4

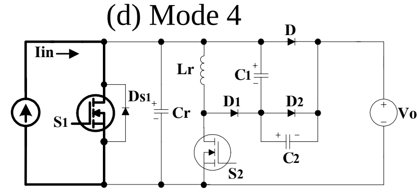

(e) Mode 5

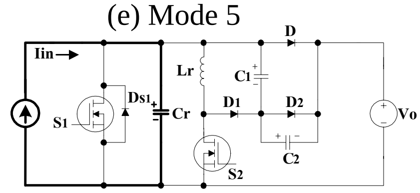

(f) Mode 6

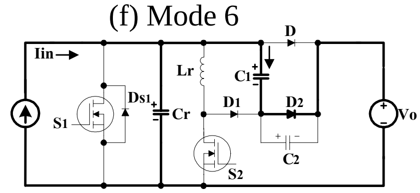

(g) Mode 7

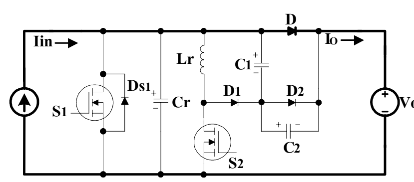

(h) Mode 8

Fig. 4. Equivalent circuit of each operation mode

$$V_{C1} = Z_n I_{Lr}(t_2)\sin\omega_n(t-t_3) \quad (7)$$

where $Z_n = \sqrt{\dfrac{L_r}{C_1+C_2}}$ $\omega_n = \dfrac{1}{\sqrt{L_r(C_1+C_2)}}$.

Mode 5 [$t_4 - t_5$]: During this period, the inductor L is charged by the input dc voltage source V_{in} while the main switch S_1 continues to be turned-on and the auxiliary switch S_2 is turned off.

Mode 6 [$t_5 - t_6$]: At t_5, the main switch S_1 begins to turn-off, the inductor L charges the resonant capacitor C_r and the voltage across the capacitor increases. The current L_r equals zero and the voltage across C_r is given by:

$$V_{Cr} = \frac{I_{in}}{C_r}t = \frac{I_L}{C_r}t. \quad (8)$$

Mode 7 [$t_6 - t_7$]: When the increasing voltage across C_r is greater then ($V_o + V_{C1}$), the capacitor C_1 begins to discharge through the diode D_2. This discharge of C_1 can slow down the rising voltage slope of the rising voltage across C_r or the main switch S_1. Therefore, the capacitor is performing as a turned-off snubber for the main switch to suppress the turned- off voltage spike and the turned-off voltage slope of the main switch S_1. The voltage across C_r is given by:

$$V_{Cr} = V_o + V_{C1} \quad (9)$$

Mode 8 [$t_7 - t_0$]: This stage begins when the diode D is turned-on under ZVS. The operation of the circuit at this stage is identical to the normal turned off operation of a PWM boost converter. It ends at the moment that S_2 is turned on to begin a new switching cycle.

Delay Time

To ensure proper operation of the ZVT soft-switching boost PFC converter, a minimum delay time (T_D) of the auxiliary switch S_2 is required. This delay time (T_D) must satisfy the following condition:

$$T_D \geq \frac{I_{in}L_r}{V_o} + \frac{\pi}{2}\sqrt{L_r C_r} \quad (10)$$

Design Procedure

In the design of a boost PFC converter, the required input power factor and the total harmonic distortion (THD) of the line current under specified ranges of line voltage is the major design goal. This design procedure of the proposed ZVT PWM boost PFC converter is summarized as follows:

Switching Frequency (f_s)

Determination of switching frequency plays a most important role in the design of the power converter. There are many factors influence its proper selection. However, the determination of switching frequency is still a compromise between theoretical analysis and practical implementation.

Peak Inductor Current ($\bar{I}_L$)

According to the design rating of the boost PFC converter, the converter was designed to operate in a continuous conduction mode, therefore, the peak inductor current is determined by:

$$V_s \bar{I}_L \frac{1}{\sqrt{2}}\eta = V_{dc} I_o = P_o \quad (11)$$

$$\bar{I}_L = \sqrt{2}\eta\frac{P_o}{V_s} \quad (12)$$

where η is the converter efficiency.

Minimum Duty Ratio (D_{min})

The minimum duty ratio occurs when the input voltage gets the maximum and this is equal to:

$$D_{min} = \frac{V_o - \bar{V}_{in(max)}}{V_o} \quad (13)$$

Primary Input Inductor (L)

The primary input inductor must satisfy a constraint governing to meet the requirement on maximum allowable ripple current. The input inductor (L) is given by:

$$L = \frac{\bar{V}_{in(min)} D_{min} T_s}{\Delta I_{in}} \tag{14}$$

where ΔI_{in} is the input ripple current and $T_s = \frac{1}{f_s}$

Output Capacitor (C_o)

The selection of the output capacitor depends on the output ripple voltage (ΔV_o) as follows:

$$C_o \geq \frac{P_o}{2\omega_s V_o \Delta V_o} \tag{15}$$

where $\omega_s = 2\pi f_{line}$

Delay Time (T_D)

The on-time of auxiliary switch (S_2) must be shorter than one tenth of the switching period.

$$T_D = \frac{1}{10} T_s \tag{16}$$

Current Stress Factor (a)

The current stress factor of the auxiliary switch is defined as

$$a = \frac{I_{Lr(pk)}}{\bar{I}_{in(max)}} \tag{17}$$

It is greater than one ($1 \leq a \leq 1.5$) and is desired to be as small as possible. This factor can be used for the selection of the auxiliary switch.

Resonant Capacitor (C_r)

The resonant capacitor (C_r) can be expressed as

$$C_r = \frac{(a-1)^2 \bar{I}_{in(max)} T_D}{V_o \left[1 + \frac{\pi}{2}(a-1)\right]} \tag{18}$$

Resonant Inductor (L_r)

The resonant inductor is given by

$$L_r = \frac{V_o T_D}{\bar{I}_{in(max)} \left[1 + \frac{\pi}{2}(a-1)\right]}. \tag{19}$$

Additional Capacitor (C_1, C_2)

To guarantee a soft-switching of the auxiliary switch, the required capacitance C_1 should be selected according to the expression:

$$C_1 < \frac{L_r \left[\bar{I}_{in(min)} + V_o \sqrt{L_r / C_r}\right]^2}{V_o^2} - C_2 \tag{20}$$

where $C_2 < C_1$.

The specifications of the prototype boost PFC converter are given in Table 1.

Table 1. Specifications of the boost PFC converter

Output power (P_o)	500 W
Output dc voltage (V_o)	400 V
Input ac voltage (V_{in})	176-264 V_{rms}
Switching frequency (f_s)	40 kHz
Output voltage ripple (ΔV_o)	5 %
Input current ripple (ΔI_{in})	20 %
Estimated efficiency (η)	$\geq$95%

Experimental Results

A 500 W, 40 kHz prototype of the proposed ZVT PWM boost PFC converter, as shown in Fig.2, has been built in the laboratory to experimentally verify the analysis. The major parameters and components are given in Table 2.

Table 2. Components used in prototype

Component	Value/Model
Switches (S_1, S_2)	IRFP450
Diode (D, D_1, D_2)	MUR8100E
Boost inductor (L)	2 mH
Resonant capacitor (C_r)	1.8 nF
Resonant Inductor (L_r)	80 μH
Output capacitor (C_o)	220 μF
Capacitor C_1	4.7 nF
Capacitor C_2	1.5 nF
Controller chip	UC3855AN

For comparison, a conventional ZVT boost PFC converter with the same specifications is also built.

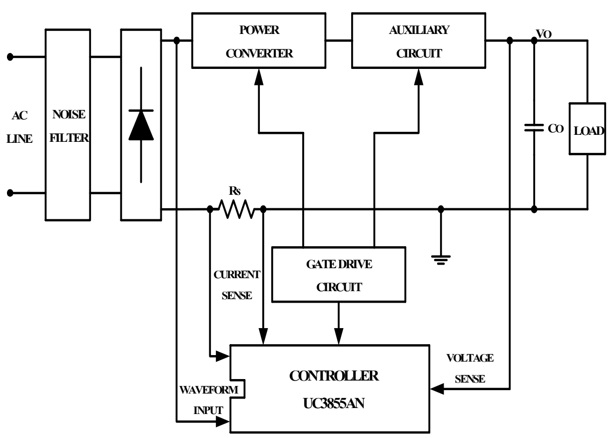

Fig. 5. Block diagram of an experimental circuit

Fig. 5 shows the block diagram of an experimental circuit. It consists of a noise filter, a diode bridge, a power converter, auxiliary circuits, gate drive circuits and a controller chip. A noise filter is used to reduce noise components in the input side. An auxiliary circuit is used to soften switching configuration. And a gate drive circuit splits a gate signal of the controller into two, where one is main circuit and other is for the auxiliary circuit. Its switching frequency is constant.

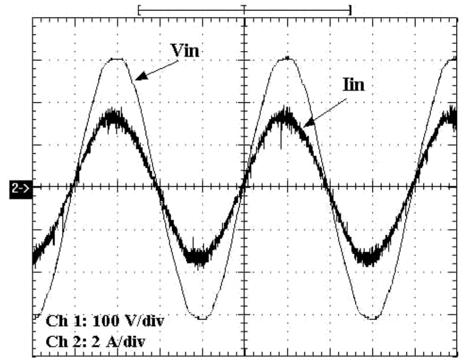

Fig. 6. Experimental results of the input voltage and current for the conventional ZVT PWM boost PFC converter, t = 5ms/div

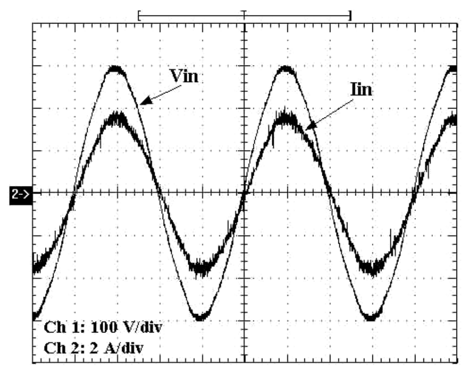

Fig. 7. Experimental results of the input voltage and current for the proposed ZVT PWM boost PFC converter, t = 5ms/div

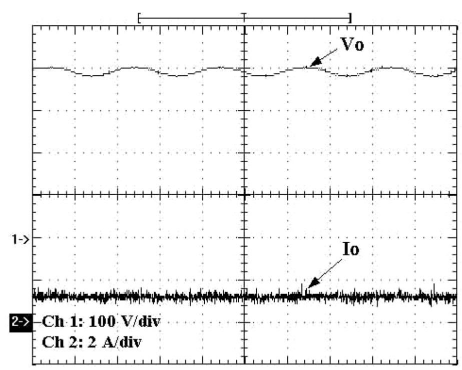

Fig. 8. Experimental results of the output voltage and current for the proposed ZVT PWM boost PFC converter, t = 5 ms/div

Fig. 6 and Fig. 7 show the waveforms of the input line voltage and line current for the conventional converter and the proposed converter. The line current is in phase with the line voltage and it is nearly sinusoidal. The power factor of both converters are almost unity (0.992) and total harmonic distortion (THD) is 2.82%. Fig. 8 shows the waveforms of the output voltage and current for the proposed converter.

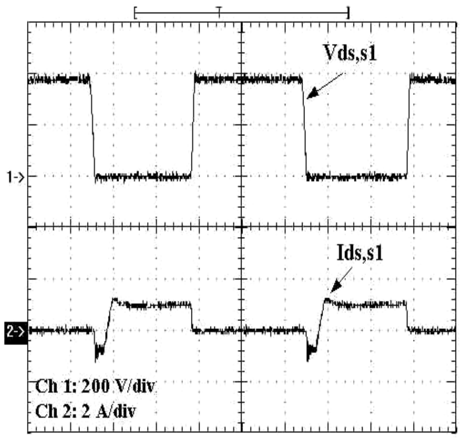

Fig. 9. Current and voltage waveforms of s_1 for the conventional ZVT PWM boost PFC converter, t = 5μs/div

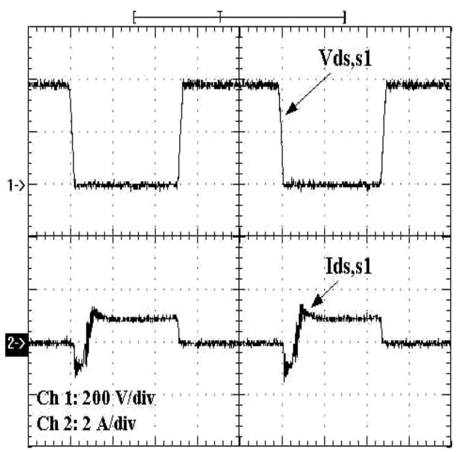

Fig. 10. Current and voltage waveforms of s_1 for the proposed ZVT PWM boost PFC converter, t = 5μs/div

Figs. 9 and 10 show the waveforms of the main switch s_1 for the conventional converter and the proposed converter. As can be seen in these figures, s_1 turns-on and turns-off under zero voltage condition.

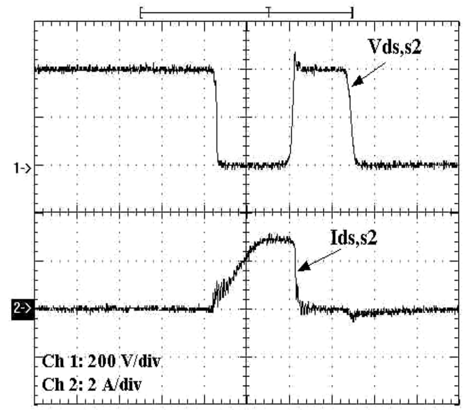

Fig. 11. Current and voltage waveforms of s_2 for the conventional ZVT PWM boost PFC converter, t = 1μs/div

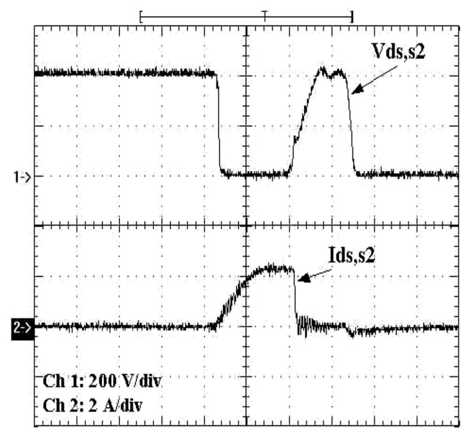

Fig. 12. Current and voltage waveforms of s_2 for the proposed ZVT PWM boost PFC converter, t= 1μs/div

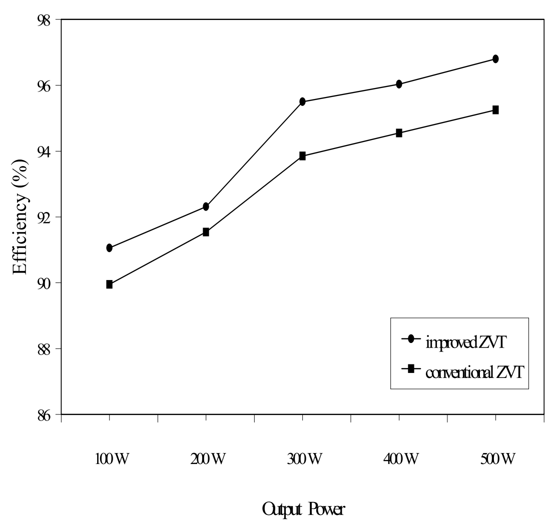

Fig. 13. Efficiency comparison between both converters

Fig. 11 shows the waveforms of the auxiliary switch s_2 for the conventional ZVT PWM boost PFC converter and the auxiliary switch is turned-on with ZCS and turned-off with hard-switching.

Fig. 12 shows the waveforms of the auxiliary switch s_2 for the proposed ZVT PWM boost PFC converter. As can be seen Fig. 12, the auxiliary switch s_2 is turned-on with ZCS and turned-off near ZVS. Thus the switching loss of s_2 is reduced. Fig.13 shows the efficiency measurements of the improved ZVT and the conventional ZVT PWM boost PFC converter (Hua, *et al.*1994). The measured efficiency at 500 W of the proposed ZVT PWM boost PFC converter is 97% as compared with the conventional ZVT PWM boost PFC converter which has an efficiency of 95 %.

Conclusion

In this paper, an improved ZVT PWM boost PFC converter was proposed. The switching loss of the auxiliary switch are minimized by using an additional circuit applied to the auxiliary switch. Besides the main switch ZVS turned-on and turned-off, and the auxiliary switch ZCS turned-on and turned-off near ZVS. Since the active switch is turned-on and turned-off softly, the switching losses are reduced and the higher efficiency of the system is achieved.

A prototype of a 500W/40 kHz system was implemented to experimentally verify the improved performance.

Acknowledgment

The author acknowledges the financial support from the Rajamangala University of Technology Isan, Sakon Nakhon Campus, Sakon Nakhon, Thailand, during a period of this work.

References

Akagi, H. 1994. Trends in active power line conditioners. IEEE Trans. Power Electronics 9: 263-8.

Bose, B.K. 1992. Power electronics - a technology review. Proc. IEEE Int. Conf. Power Electronics (PESC'92), pp. 1303-34.

Gegner, J.P.; and Lee, C.Q. 1994. Zero-voltage -transition converters using an inductor feedback technique. Proc. IEEE Int. Conf. Power Electronics (PESC'94), pp. 590-6.

Hua, G.; Leu, C. S.; Jiang, Y.; and Lee, F. C. 1994. Novel zero-voltage-transition PWM converter. IEEE Trans. Power Electronics 9: 213-9.

Kaewarsa, S.; Krongkitsiri, W.; Prapanavarat, C.; and Yangyuen, U. 2004. An improved ZVT-PWM DC-DC boost converter using additional circuit. Proc. IEEE Int. Conf. TENCON 2004, pp. 201-4.

Kim, T.W.; Kim, H.S.; and Ahn, H.W. 2000. An improved ZVT PWM boost converter. Proc. IEEE Int. Conf. Power Electronics (PESC'00), pp. 615-9.

McEachern, W. 1990. Power electronics in the 1990's. Proc. IEEE Int. Conf. Industrial Electronics (IECON'90), pp. 839-43.